Large-Scale Motions and Electrostatic Properties of Furin and HIV-1 Protease[†]

V. Carnevale, S. Raugei, C. Micheletti, and P. Carloni*

International School for Advanced Studies and CNR-INFM Democritos, Via Beirut 2-4, I-34014 Trieste, Italy

Received: July 3, 2007; In Final Form: October 4, 2007

We present a comparative study between two members of serine and aspartic proteases complexed with a peptide substrate. The same computational setup is used to characterize the structural, electrostatic, and electronic properties for the Michaelis complex of furin, a serine protease, and of the aspartic protease from HIV-1. In both cases plane-wave density functional theory (PW-DFT) and empirical force-field-based molecular dynamics calculations are used. For furin, calculations are extended to the complex with the intermediate of the first step of the reaction. Comparisons are also made with results from recent PW-DFT investigations on both families of enzymes and with the same chemical groups in an aqueous environment. It is found that the substrate carbonyl group is more polarized in the furin complex than in the HIV-1 protease one. A further difference regards the large-scale motions of the complexes as a whole and local conformational fluctuations at the active site. The global and local fluctuations are well coupled for HIV-1 protease but not for furin. Thus, despite some chemical analogies in the first step of the reaction mechanism, furin and HIV-1 protease complexes appear to be characterized by a different interplay of electrostatics and conformational fluctuations.

Introduction

Atomistic molecular dynamics (MD) simulations as well as mesoscopic approaches have highlighted the general importance of concerted structural fluctuations for the internal dynamics of enzymes.[1−15] Owing to their important role in the cell cycle of all living organisms[16] proteolytic enzymes have been an early target for these dynamics-based investigations.[3,9,17−19] Only recent MD simulations, however, have shown that two proteases with distinct folds (HIV-1 protease and β-secretase) possess similar large-scale concerted movements modulating the active site geometry.[3,19]

The introduction of suitable coarse-grained models has broadened the scope of the atomistic approaches by enabling the systematic characterization of collective movements for representatives of the entire superfamily of proteolytic enzymes.[20] It was found that several proteases, differing by folds and catalytic chemistry, can nevertheless sustain similar large-scale concerted movements.[20] An exception to this pervasive and remarkable overall accord of concerted movements is constituted by aspartic and serine proteases (APs and SPs hereafter).[20] Their low degree of similarity stimulated the present study, which compares, for the two systems, aspects related to electrostatics and conformational fluctuations.

The comparison of serine and aspartic proteases is made particularly interesting by the fact that the first step of their catalytic cycle shows nontrivial chemical similarities.[21−25] Indeed, the first stage of this multistep hydrolysis reaction involves a nucleophilic attack toward the substrate carbonyl group. The attack is performed by a serine[26] in SP's and a water molecule[3,17−19,27] in AP's (E-S in Figure 1). Both nucleophiles interact by H-bond donor functionalities (stronger for water), which might modify their nucleophilic power relatively to the bulk aqueous environment. The nucleophilic attack leads to the
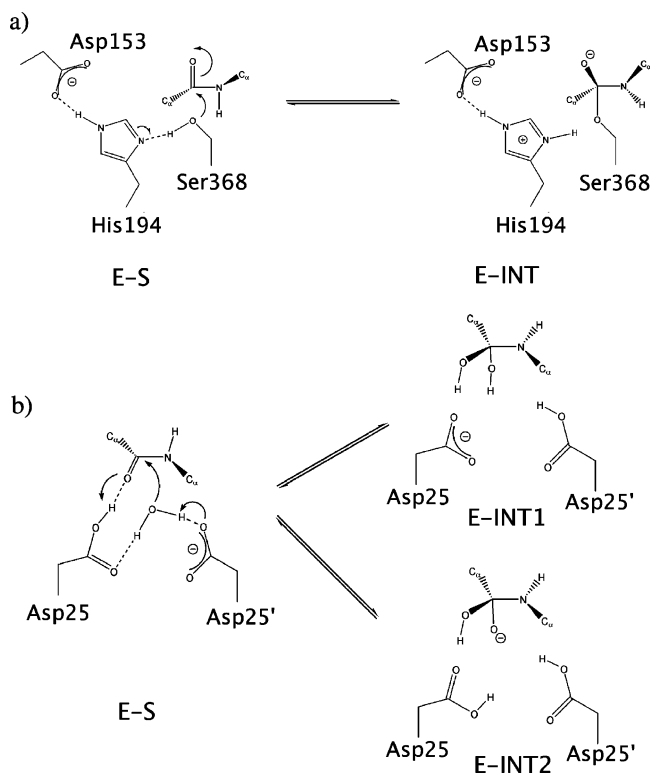
Figure 1. Scheme of the first step of the hydrolysis reaction catalyzed by serine proteases[23] (a) and asparic proteases[21] (b). In (a) the catalytic serine residue (Ser368 in furin, the serine protease considered in this work) performs a nucleophilic attack on the carbonyl carbon of the substrate, with the formation of a negatively charged tetrahedral intermediate. In (b) a water molecule, H-bonded to the catalytic Asp dyad, performs a nucleophilic attack on the carbonyl carbon of the substrate forming a highly reactive intermediate. The latter has been proposed to be either neutral[30] (E-INT1) or negatively charged[27](E-INT2). Residue numbers refer to those of HIV-1 PR, the aspartic protease investigated here.

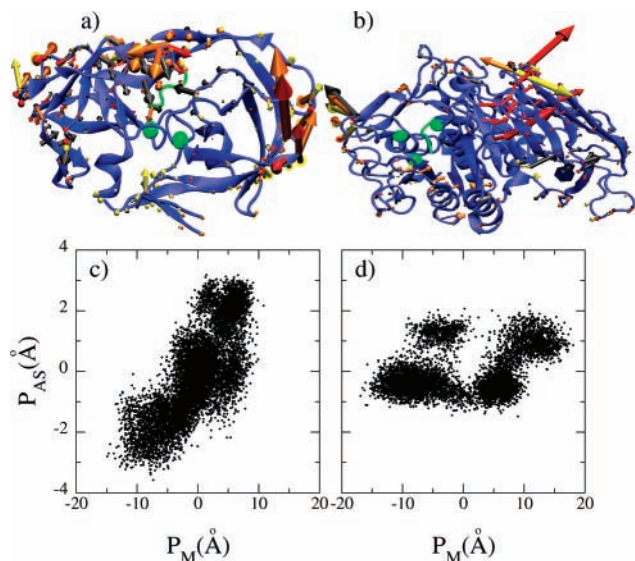**12328** *J. Phys. Chem. A, Vol. 111, No. 49, 2007*

Carnevale et al.

Figure 2. Upper panels: HIV-1 PR (a) and furin (b) Michaelis complexes (E-S). The top four eigenvectors of the covariance matrix are represented as arrows of width and length proportional to the modulus. The first, second, third, and fourth eigenvectors are colored in red, gray, orange, and yellow, respectively. Active site residues and the substrate are highlighted in green. Bottom panels: Equal time projections of the instantaneous conformational fluctuations along the first essential dynamical space for the whole Michaelis complexes (P_M) and for the active site regions (P_{AS}) of HIV-1 PR (c) and furin (d).

formation of a negatively charged transition state (TS) for SP's,[23-25] stabilized by the electric field of the active site,[26,28] and, subsequently, to a negatively charged intermediate (E-INT in Figure 1a). For AP's, instead, two alternatives have been proposed: either a negatively charged tetrahedral intermediate[27] or a neutral one[3,18,19] (E-INT1 and E-INT2 in Figure 1b).

To investigate similarities and differences between serine and aspartic proteases, we compare, within the same computational setup, structural and electronic properties of the Michaelis complexes (E-S) for two specific enzymes: furin,[29] an α/β monomeric SP member and the mainly-β dimeric AP from human immunodeficiency virus HIV-1 PR (Figure 2a,b). For the latter we perform novel analysis on data collected by our group in previously published QM/MM and classical MD studies.[18,19,30] For furin, the investigation is extended to the complex with the negatively charged INT species (Figure 1a), whose existence was established by previous calculations[26,28] as well as experimental work.[23] Although enzymes clearly stabilize the TS (and not the intermediate) relatively to the Michaelis complex, calculations on the E-INT complex might provide insights on the mechanism, as in SP's the reaction proceeds through late-TS.[31] Data from simulations of simple systems such as bulk water[32] and ethanol in water solution[33] are used here as reference systems for the nucleophilic agents.

The calculations provide new elements regarding the reactants polarization. It is found that the substrate carbonyl group in the furin complex is more polarized than that in the HIV-1 PR one. On the other hand, for the nucleophiles we found that the catalytic water in HIV-1 PR is more polarized than in the bulk, whereas the opposite is true for the catalytic serine in furin. A further salient difference concerns large-scale conformational fluctuations. The global concerted movements do not appreciably modulate the active site geometry in furin, whereas they significantly couple to the active site conformational fluctuations in HIV-1 PR.

Thus, although the first step of the proteolytic reaction mechanism of furin and HIV-1 protease share some common traits, the two enzymes exhibit a different interplay of electrostatics and conformational fluctuations.

Materials and Methods

Furin. The E-S and E-INT models are based on the structure of mouse-furin ectodomain (residues 108−578) covalently bound to the tetrapeptide inhibitor decanoyl-Arg-Val-Lys-Arg-chloromethylketone (pdb code: 1P8J).[29] This inhibitor, which contains the consensus sequence for furin cleavage, is slightly modified to generate a functional substrate for the enzyme (acetyl-Arg-Val-Lys-Arg-*N*-methyl).[34] In E-S, Asp153 and His194 are assumed to be charged and δ-protonated, respectively.[31] In E-INT the O_γ of the serine is bound to the carbonyl carbon of the scissile peptide bond and Asp153 and His194 are assumed to be both in their charged state.[23-25] E-S and E-INT are immersed in a rectangular box containing 17 365 water molecules. Their overall negative charge is neutralized by adding 5 sodium ions, located far from the active site to minimize their electrostatic effect on the reactants.

Constant temperature[35] and constant pressure[36] MD simulations are performed with the GROMACS package[37] using the AMBER parm94 force field.[38] For E-INT, all the tetrahedral intermediate parameters were taken from the general AMBER force field (GAFF), whereas point charges were obtained following the standard procedure adopted in AMBER force field.[38] Periodic boundary conditions are applied by treating long-range electrostatic interactions with the particle-mesh Ewald technique.[39] A time step of 1.5 fs is used with all bond lengths kept fixed by applying LINCS algorithm.[40] The time evolution of the system is followed for 10 ns, after an equilibration period of 0.5 ns at 310 K and 1 bar. Electrostatic effects are calculated carrying out QM/MM hybrid Car−Parrinello DFT based molecular dynamics simulations on the E-S complex using the CPMD3.10/Gromos code.[41] The calculations are performed employing the BLYP[42,43] gradient-corrected exchange and correlation energy functional, along with a plane wave expansion of the valence electrons wavefunctions[44] with a cutoff of 70 Ry and Troullier−Martins pseudopotentials.[45] The QM region contains the catalytic residues (Asp153, His194, and Ser368) and the scissile peptide bond. Hydrogen atoms are added to saturate the bonds at the interface between the QM region and the MM one. The rest of the system is treated using the same force field as in classical MD simulation (AMBER parm94 force field[38]). The calculations were started from the last configuration of the 10 ns long classical MD simulation and the QM/MM dynamical evolution was monitored for 3 ps (NVT ensemble).[35]

HIV-1 PR. The novel analysis on HIV-1 PR and on the reactants (bulk water and ethanol in water solution) presented here is performed on trajectories obtained previously for the E-S complex (see ref 19) using the same computational setup discussed for furin. In particular for HIV-1 PR the analysis is performed on a 10 ns trajectory from a constant temperature−constant pressure classical MD simulation performed using the same force field used for furin. Likewise, 4 ps hybrid QM/MM Car−Parrinello simulations were performed using the same gradient-corrected exchange and correlation energy functional and the same cutoff in the plane-wave expansion of the wave function. The DFT region is constituted by the catalytic residues (Asp25 and Asp25'), the scissile peptide bond and the catalytic water molecule.

Most of the presented results are based on the following analysis:

(i) Principal Component Analysis (PCA). The large-scale concerted movements of the enzymes are obtained as the top

eigenvectors of the covariance matrix **C**. The latter is obtained from the instantaneous displacement vector $\delta\vec{x}_i$ (after removal of rigid body motions) of the ith C_α atom from the reference (time-averaged) position. The matrix element $C_{i,j,\alpha,\beta}$ is, in fact, defined as $C_{i,j,\alpha,\beta} = \langle \delta x_i^\alpha \, \delta x_j^\beta \rangle$ where α and β denote the Cartesian components and the brackets indicate the time average.[46,47]

(ii) Electrostatics. Bond polarizations are obtained by analyzing the many-body wave function. As a practical descriptor we used the Boys orbitals[48] calculated as in ref 32 on 30 and 40 configurations equispaced in time, spanning the 3 and 4 ps for furin and HIV-1 PR, respectively.

As fewer computational characterizations exist for furin than HIV-1 PR, we have carried out for the former additional classical electrostatic calculations. Specifically, the classical MD trajectory was used to obtain the electrostatic interaction energy between residues at the catalytic site and their surrounding protein/solvent environment. It should be pointed out that the resulting electrostatic description in terms of effective point charges has not the same transparency and reliability as quantum calculations. In the present context it will therefore be used to draw only qualitative conclusions.
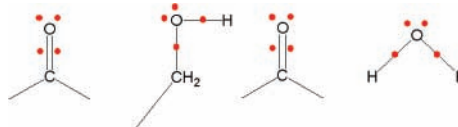
Results and Discussion

The results of our investigations for the HIV-1 protease and furin are hereafter presented in a comparative fashion. The material has been organized so as to cover the salient properties of the conformational fluctuations of the Michaelis complexes (E-S). For furin the discussion is extended to the structural characterization of Michaelis complex and of the first reaction intermediate. Finally, we provide a discussion on the electrostatic field at the active site.

HIV-1 PR Michaelis Complex: Structures and Conformational Fluctuations. To investigate the role of conformational fluctuations for the enzymatic reaction, we monitored the time evolution of the sum of the distances between the C_α atoms of the substrate and those of the catalytic Asp's (the sum involves four atom pairs in total). These distances show two abrupt changes, which correspond to the forward and reverse transition from an average distance of 7.5 Å to an average distance of 8.5 Å occurring respectively after 0.8 and 1.8 ns of the simulated evolution (10 ns in total). Previous ab initio calculations, aimed at clarifying the reaction mechanism of this protease, demonstrated that only one of these two active site conformations is capable of catalyzing the proteolytic reaction[3,30] and showed a role for global conformational fluctuations in modulating these conformational transitions.

To ascertain if the global conformational fluctuations of the complex as a whole are capable of modulating the active site region, we performed and compared two principal component analyses (PCA's). The first analysis was performed over the entire enzyme/substrate complex, and the second was restricted to the active site region. We define the latter as comprising all residues at a distance smaller than 10 Å from the catalytic Asp25 (the distance was measured between the C_α atoms). This criterion lead to the selection of 23 residues defining the active site region.

The top eigenvectors of the covariance matrix (essential dynamical spaces) calculated for the whole complex were found to have a significant norm on the active site region, particularly on the flaps, suggesting a strong mechanical coupling between the active site and the rest of the protein (see Figure 2a). The strength of this mechanical coupling is conveyed by the scatter plot of Figure 2c where we have represented the instantaneous

TABLE 1: Electronic Structure of the Reactive Groups Involved in the Peptide Hydrolysis Reaction in HIV-1 PR and Furin[a]

furin   HIV-1 PR

	furin	HIV-1 PR	ethanol	bulk water
$d(\text{O}_{\text{Pep}}-\text{BO}^1_{\text{lone}})$	0.33	0.34		
$d(\text{O}_{\text{Pep}}-\text{BO}^2_{\text{lone}})$	0.31	0.32		
$d(\text{C}_{\text{Pep}}-\text{BO}^1_{\text{C=O}})$	0.88	0.86		
$d(\text{C}_{\text{Pep}}-\text{BO}^2_{\text{C=O}})$	0.89	0.88		
$d(\text{O}_{\text{Pep}}-\text{BO}^1_{\text{C=O}})$	0.47	0.48		
$d(\text{O}_{\text{Pep}}-\text{BO}^2_{\text{C=O}})$	0.47	0.47		
$d(\text{O}_{\text{Hyd}}-\text{BO}^1_{\text{lone}})$	0.31		0.33	
$d(\text{O}_{\text{Hyd}}-\text{BO}^2_{\text{lone}})$	0.31		0.32	
$d(\text{O}_{\text{Hyd}}-\text{BO}_{\text{O}-\text{H}})$	0.50		0.50	
$d(\text{O}_{\text{Hyd}}-\text{BO}_{\text{C}-\text{O}})$	0.57		0.55	
$d(\text{O}_{\text{Wat}}-\text{BO}^1_{\text{lone}})$		0.32		0.33
$d(\text{O}_{\text{Wat}}-\text{BO}^2_{\text{lone}})$		0.33		0.33
$d(\text{O}_{\text{Wat}}-\text{BO}_{\text{O}-\text{H1}})$		0.47		0.50
$d(\text{O}_{\text{Wat}}-\text{BO}_{\text{O}-\text{H2}})$		0.53		0.50

[a] Bottom: distances (in Å) of the center of selected Boys orbitals (BO's) from selected atoms in the active site of furin and HIV-1 PR and of the corresponding nucleophiles (ethanol and water) in aqueous solution. Distances are reported for: (i) the hydroxyl group of Ser368 and the carbonyl group of the scissile peptide bond for furin; (ii) the catalytic water molecule and the carbonyl group of the scissile peptide bond for HIV-1 PR. Top: picture of the BO's considered for furin and HIV-1 PR.

amplitude of the system motion projected (at equal times) on the first essential eigenvector of (i) the entire complex and (ii) of the active site region. The essential eigenvector and the amplitudes of the projected motion are calculated after removal of the rigid body motion of (i) the whole complex and (ii) the active site region. The plot therefore provides a visual perception of the high degree of correlation between the fluctuation dynamics of the complex as a whole and that of the active site region.

Furin: Structures and Dynamics of E-S and E-INT. The MD-averaged distances among active site atoms in the two species are very similar to those calculated from the X-ray structure (Table 1, Supporting Information). In both cases, the initial active site H-bond pattern involving the catalytic triad (Asp153-His194-Ser368, Table 1, Supporting Information) is preserved all along the MD trajectory. There are, however, significant differences in the active site geometry (Table 1, Supporting Information). (i) Asn295 residue, which constitutes the so-called oxyanion hole and is fully conserved in subtilisin-like serine proteases,[23,49] points toward the solvent in E-S, whereas it forms an H-bond interaction with the substrate. (ii) The number of H-bonds between the catalytic triad and three of the substrate residues (Arg2, Nme4, and Arg5) is larger in E-INT than in E-S (Figure 3). In particular, the carbonyl oxygen of Arg5, which is hydrogen-bonded to Asn295 in E-INT, in E-S is found to be H-bonded to a water molecules coming from the bulk. The difference in H-bond interactions is also supported by the calculation of the E-INT and E-S electrostatic interaction energy, which in the AMBER force field takes into account H-bonding interactions.[38] As can be seen from Figure 4, the electrostatic stabilization of E-INT is larger than that of E-S. These observations are consistent with a previous QM/MM investigation on trypsin,[31] which showed that the electrostatic
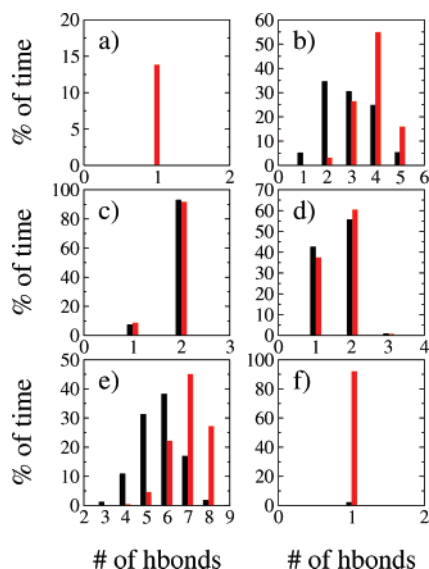
Figure 3. MD of furin: normalized distributions (black, E-S; red, E-INT) of the number of H-bonds involving the Ace-RVKR-Nme substrate investigated in this study: (a) Ace1; (b) Arg2; (c) Val3; (d) Lys4; (e) Arg5; (f) Nme6.
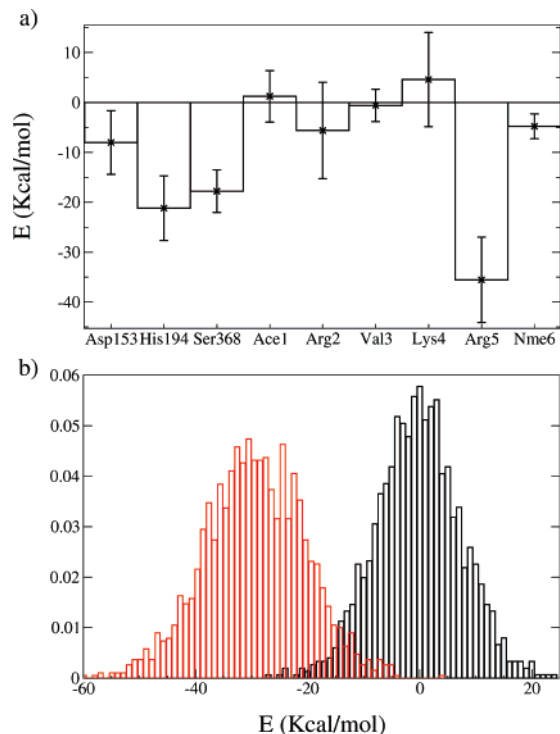

Figure 4. Interactions in furin: (a) difference, between E-S and E-INT, in the electrostatic interaction energy between each residue and the rest of the system (standard deviations are represented as error bars); (b) normalized distribution of the total interaction energy between the active site and the rest of system (black, E-S; red, E-INT). The obtained electrostatic energies should be taken only for a qualitative comparison.

interaction energy between the active site and the protein environment is more negative for E-INT than for E-S with a difference of about 20 kcal/mol (Figure 4 of ref 31) and that the carbonyl oxygen forms one H-bond in E-S and two in E-INT.

The relative distances between the C_α atoms of the substrate and those of the active site fluctuate with a rather constant dispersion around an average value of 3.1 Å with a standard deviation of 0.17 Å. Compared to the case of HIV-1 PR this motion appears to be less correlated to that of the residues in

the active site. As for the HIV-1 PR case, this region is defined as the set of 24 residues for which the distance of the C_α atom from the C_α atom of the catalytic His194 is smaller than 10 Å.

The top eigenvectors of the covariance matrix calculated on the whole complex do not show a significant norm on residues belonging to the active site pocket (see Figure 2b). This contrasts to what observed in HIV-1 PR (Figure 2a). Notably, also the coupling between the active site motion and that of the whole complex is much less pronounced than in the case HIV-1 PR. This is readily perceived in the scatter plot of Figure 2d which, analogously to the Figure 2c, provides the amplitudes at equal times of the motion projected along the first essential eigenvector of the whole complex versus the one of the active site region.

In summary, conformational fluctuations at the furin active site have a smaller amplitude (by a factor 2) compared to HIV-1 PR (see Figure 2d) and are more weakly coupled to the global concerted motions of the complex.

Polarization of the Reactants in the Michaelis Complexes. We extended the investigations presented above to analyze the influence of the protein electrostatic field. To this end, DFT calculations on furin were performed here, whereas for HIV-1 PR we relied on data previously collected by our group.[30] For completeness, comparisons with models of nucleophilic agents in aqueous solution have also been carried out. Specifically, ethanol in water[33] and bulk water[32] were used for SP's and AP's, respectively.

The electronic structure of functional groups involved in the reaction is characterized in terms of Boys orbitals (BO's),[48] which permits an expansion of the many-body wave function onto doubly occupied orbitals corresponding to covalent bonds and lone pairs. The center of charge of the BO (BOC) provides a useful tool to quantify the polarization of covalent bonds and to analyze differences in the electronic structure of the same functional group in different environments.

We first discuss the polarization of the nucleophilic agents. In furin, the serine hydroxyl group donates a hydrogen bond to His194 and does not receive any H-bond from the surrounding residues. Instead, in solution two water molecules are H-bonded to the hydroxyl oxygen of ethanol. As a result, an appreciable shift of electron density from the carbon atom to the oxygen atom and a displacement of the lone pairs BOC's (see Table 1) takes place. This is an indication of a larger polarization of the hydroxyl moiety of ethanol in aqueous solution than of serine in the furin active site. On the other hand, the charge distribution of the nucleophilic agent in HIV-1 PR is strongly asymmetric because of the presence of the charged Asp25 to which water is bound. The BOC placed between the oxygen atom and the hydrogen atom H-bonded to the Asp25 carboxylate is systematically closer to oxygen than the one of the other water O−H bond. The difference between the two distances (0.47 and 0.53 Å, respectively) hints at the role of the carboxylate moiety in the activation of the water molecule and in the breaking of the O−H bond during the nucleophilic attack. Thus, the electronic structure of the nucleophile appears to be significantly affected by the active site environment, which, arguably, enhances the water reactivity. When the total water charge distribution is considered, this asymmetry in the electronic distribution results only in the deviation of the dipole moment vector from the molecular C_2 axis. The overall electrostatic properties, mostly determined by the molecular dipole moment, do not appreciably differ from that of bulk water (3.2 D versus 3.1 D[50]).
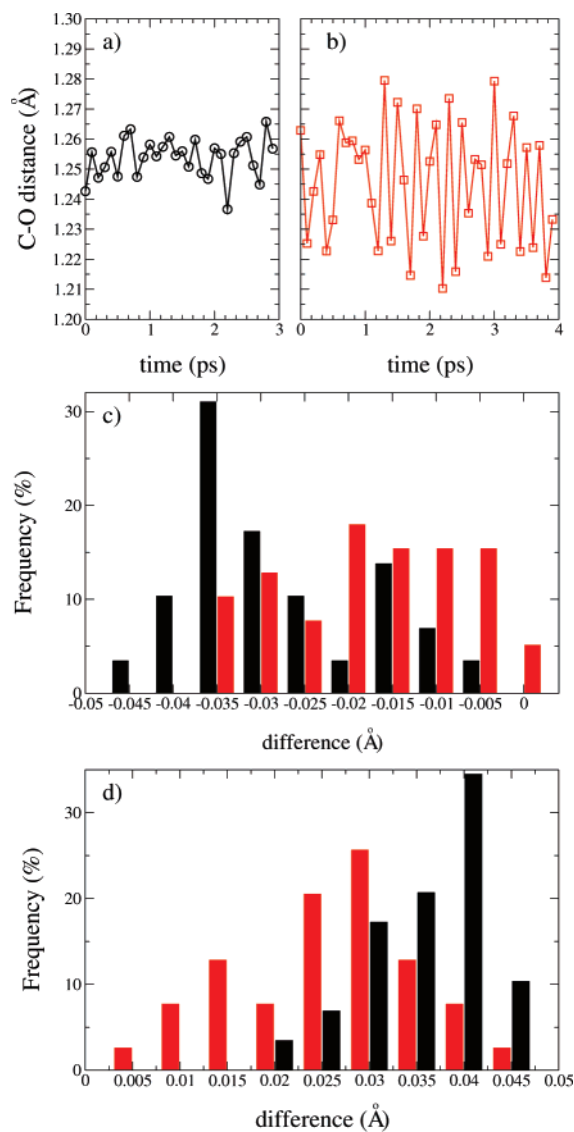
Figure 5. Comparative analysis of structural and electronic properties of furin (black) and HIV-1 PR (red) Michaelis complexes (E-S). The C=O bond length is reported, for selected configurations, as a function of time for furin (a) and HIV-1 PR (b). Displacements of C=O double bond Boys orbitals centers on going from the gas phase to the enzyme active site: (c) differences in the distance from the carbon atom to the Boys orbital centers; (d) differences in the distance from the oxygen atom to the Boys orbital centers.

The analysis of the dynamical evolution of the enzyme substrate in the two different active sites reveals that the distribution of C=O bond lengths is rather different. As shown in Figure 5a,b, the bond length in furin fluctuates in the [1.25, 1.26] Å range, whereas for HIV-1 PR the populated range is [1.22, 1.27] Å. By comparison with furin, the distribution of HIV-1 PR not only is broader but also extends toward smaller bond lengths. The bond length difference is, on average, 8.2×10^{-3} Å and the error, estimated from the semidispersion of data from the first and the second halves of the trajectories, is 10^{-3} Å. The wider spread of bond length distribution for HIV-1 PR arguably reflects the larger oscillation of the carbonyl and H-bond donor O−O distance (40% larger in HIV-1 PR than in furin). Instead, the average difference in bond lengths suggests that in furin the carbonyl carbon atom is more susceptible to the nucleophilic attack. The carbonyl bond length is, in fact, generally associated with the electrophilic character of the carbon atom.[51] In addition, bond length differences of the order

of 10^{-2} Å, as those observed here, have been experimentally associated with variations of about 10 kcal/mol in the activation barrier for the nucleophilic attack to the carbonyl carbon.[51−53]

Both aspects appear noteworthy, as in HIV-1 PR the substrate carbonyl group is hydrogen-bonded to Asp25′, which is by far more acid than the water molecule bound to the substrate carbonyl group of furin. The opposite effect on the bond lengths would be therefore expected on the basis of the chemical nature of reactive groups in the two active sites. An explanation for this fact might involve the different electrostatic interactions with the protein/solvent environment. To investigate this point, we have compared the electronic structure of the electrophile calculated in the enzyme active site with that calculated in the gas phase for the same configurations. Parts c and d of Figure 5 report the displacement of the BOC's on passing from the gas phase to the enzyme. In both enzymes a sizable displacement of the bond BOC's of the carbonyl group toward the oxygen atom results from the electrostatic interaction with the environment. In the case of furin, again, this displacement is more pronounced. This finding is consistent with the hypothesis that electrostatic interactions are responsible for the differences in electronic structure observed between furin and HIV-1 PR Michaelis complexes.

This set of observations are compatible with an opposite role of polarization of nucleophilic and electrophilic groups in the two enzymes active sites. In HIV-1 PR not only the first step of the catalytic reaction involves a stronger nucleophile, but also there are also indications that the reactivity of the catalytic water could be increased by the Asp25′ carboxylate group. In furin the presence of a weaker nucleophile might be compensated by a greater electrophilicity of the substrate carbonyl carbon atom induced by the electrostatic field of the environment.

Conclusions

We have compared structural fluctuations and electronic properties of the Michaelis complexes for two members of the protease enzymatic class: furin (a serine protease) and the HIV-1 protease (an aspartic protease). The analysis was carried out on data obtained from simulations performed for this study as well as on a novel analysis of previously calculated trajectories.[19,33] Results of DFT simulations of bulk water and ethanol in water solution have been used as reference for comparing the polarization of the reactive groups of the two enzymes. For furin, we have extended our study to the complex with the negatively charged INT. Within this single methodological framework, we compare the complexes as a transparent mean of highlighting differences in conformational fluctuations and electronic properties.

A key role for the nucleophilic power of catalytic water and serine is played by the presence of the general bases, an aspartate and a histidine, respectively. Our investigation suggests that the hydroxyl group of Ser368 in furin, which is responsible for the nucleophilic attack to the carbonyl carbon atom of the substrate, is less polarized by the protein environment than the same functional group of an ethanol molecule in aqueous solution. In contrast, in HIV-1 PR, the O−H bonds are more polarized than in the bulk. The analysis of the substrates electronic densities gives evidence that the weaker nucleophilic character of serine relative to the catalytic water in HIV-1 PR might be compensated by a larger polarization of the substrate carbonyl carbon induced by the furin environment, which increases its electrophilic character.

A further difference emerging from our investigation regards the concerted movements of the protein/substrate complex. This issue was addressed by analyzing, for both enzymes, the consistency of the local essential dynamical spaces at the active site with the global ones of the Michaelis complexes. For HIV-1 PR it is ascertained that, consistently with previous analysis,[19] the substrate/active-site modulation is mechanically assisted by the delocalized concerted movements of the complex. In contrast, no such global mechanical coupling was detected in furin whose active site, furthermore, fluctuates to a lesser extent than that of HIV-1 PR.

In conclusion our findings suggest that furin and HIV-1 PR complexes show differences in the reactants polarization and in the local/global character of conformational fluctuations modulating the active site. This appears consistent with the low degree of similarity of structure and conformational fluctuations of AP's and SP's recently emerged from a comprehensive survey of the common features shared by representatives of the proteases enzymatic class.[20] The different role of electrostatics in furin is also suggested by the observation that E-INT is more stabilized by hydrogen bonds than E-S.

The elements presented in this study complement consistently previous investigations regarding the role of conformational fluctuations for the reactivity of HIV-1 PR[3,18,19,54] and of electrostatics for that of serine proteases.[26,28]

Supporting Information Available: Table of furin distances. This material is available free of charge via the Internet at http://pubs.acs.org.

References and Notes

(1) Goh, C. S.; Milburn, D.; Gerstein, M. *Curr. Opin. Struct. Biol.* **2004**, *14*, 104−109.

(2) Bahar, I.; Atilgan, A. R.; Demirel, M. C.; Erman, B. *Phys. Rev. Lett.* **1998**, *80*, 2733−2736.

(3) Cascella, M.; Micheletti, C.; Rothlisberger, U.; Carloni, P. *J. Am. Chem. Soc.* **2005**, *127*, 3734−3742.

(4) Neri, M.; Cascella, M.; Micheletti, C. *J. Phys.: Condens. Matter* **2005**, *17*, 1581−1593.

(5) Ben-Avraham, D.; Tirion, M. M. *Physica A* **1998**, *249*, 415−423.

(6) Micheletti, C.; Carloni, P.; Maritan, A. *Proteins* **2004**, *55*, 635−645.

(7) Pontiggia, F.; Colombo, G.; Micheletti, C.; Orland, H. *Phys. Rev. Lett.* **2007**, *98*, 048102.

(8) Carnevale, V.; Pontiggia, F.; Micheletti, C. *J. Phys.: Condens. Matter* **2007**, In press.

(9) Tousignant, A.; Pelletier, J. N. *Chem. Biol.* **2004**, *11*, 1037−1042.

(10) McCammon, J. A.; Gelin, B. R.; Karplus, M.; Wolynes, P. G. *Nature* **1976**, *262*, 325−326.

(11) Swaminathan, S.; Ichiye, T.; van Gusteren, W.; Karplus, M. *Biochemistry* **1982**, *21*, 5230−5241.

(12) Brooks, B.; Karplus, M. *Proc. Natl. Acad. Sci. U.S.A.* **1985**, *82*, 4995−4999.

(13) Sulpizi, M.; Rothlisberger, U.; Carloni, P. *Biophys. J.* **2003**, *84*, 2207−2215.

(14) Miyashita, O.; Onuchic, J. N.; Wolynes, P. G. *Proc. Natl. Acad. Sci. U.S.A.* **2003**, *100*, 12570−12575.

(15) Chennubhotla, C.; Bahar, I. *Mol. Syst. Biol.* **2006**, *2*, 36.

(16) Tyndall, J. D.; Nall, T.; Fairlie, D. P. *Chem. Rev.* **2005**, *105*, 973−999.

(17) Zhang, Y.; Kua, J.; McCammon, J. A. *J. Phys. Chem.* **2003**, *107*, 4459−4463.

(18) Piana, S.; Carloni, P.; Rothlisberger, U. *Protein Sci.* **2002**, *11*, 2393−2402.

(19) Piana, S.; Carloni, P.; Parrinello, M. *J. Mol. Biol.* **2002**, *319*, 567−583.

(20) Carnevale, V.; Raugei, S.; Micheletti, C.; Carloni, P. *J. Am. Chem. Soc.* **2006**, *128*, 9766−8772.

(21) James, M. N. G. In *Catalytic pathway of aspartic peptidases. In Handbook of Proteolytic Enzymes*, 2nd ed.; Barrett, A. J., Rawlings, N. D., Woessner, J. F., Eds.; Elsevier: London, 2004; pp 12−19.

(22) Northrop, D. B. *Acc. Chem. Res.* **2001**, *34*, 790−797.

(23) Rawlings, N. D.; Barrett, A. J. In *Introduction: serine peptidases and their clans. In Handbook of Proteolytic Enzymes*, 2nd ed.; Barrett, A. J., Rawlings, N. D., Woessner, J. F., Eds.; Elsevier: London, 2004; pp 1417−1439.

(24) Hedstrom, L. *Chem. Rev.* **2002**, *102*, 4501−4523.

(25) Daggett, V.; Schroeder, S.; Kollman, P. *J. Am. Chem. Soc.* **1991**, *113*, 8926−8935.

(26) Warshel, A. *J. Biol. Chem.* **1998**, *273*, 27035−27038.

(27) Aqvist, J.; Warshel, A. *Chem. Rev.* **1993**, *93*, 2523−2544.

(28) Warshel, A.; Naray-Szabo, G.; Sussman, F.; Hwang, J. K. *Biochemistry* **1989**, *28*, 3629−3637.

(29) Henrich, S.; Cameron, A.; Bourenkov, G. P.; Kiefersauer, R.; Huber, R.; Lindberg, I.; Bode, W.; Than, M. *Nat. Struct. Biol.* **2003**, *10*, 520−526.

(30) Piana, S.; Bucher, D.; Carloni, P.; Rothlisberger, U. *J. Phys. Chem. B* **2004**, *108*, 11139−11149.

(31) Ishida, T.; Kato, S. *J. Am. Chem. Soc.* **2003**, *125*, 12035−12048.

(32) Silvestrelli, P. L.; Parrinello, M. *Phys. Rev. Lett.* **1999**, *82*, 3308.

(33) Erp, T. S. V.; Meijer, E. J. *J. Chem. Phys.* **2003**, *118*, 8831.

(34) Krysan, D. J.; Rockwell, N. C.; Fuller, R. S. *J. Biol. Chem.* **1999**, *274*, 23229−23234.

(35) Nosé, S. *J. Chem. Phys.* **1984**, *81*, 511−519.

(36) Parrinello, M.; Rahman, A. J. *J. Appl. Phys.* **1981**, *52*, 7182−7190.

(37) van der Spoel, D.; Lindahl, E.; Hess, B.; Groenhof, G.; Mark, A.; Berendsen, H. J. C. *J. Comput. Chem.* **2005**, *26*, 1701−1718.

(38) Cornell, W.; Cieplak, P.; Bayly, C.; Gould, I.; Merz, K. J.; Ferguson, D.; Spellmeyer, D.; Fox, T.; Caldwell, J.; Kollman, P. *J. Am. Chem. Soc.* **1995**, *117*, 5179.

(39) Essmann, U.; Perera, L.; Berkovitz, M. L.; Lee, T. D. H.; Pedersen, L. G. *J. Chem. Phys.* **1995**, *103*, 8577−8593.

(40) Hess, B.; Bekker, H.; Berendsen, H. J. C.; Fraije, J. G. E. M. *J. Comput. Chem.* **1997**, *18*, 1463−1472.

(41) Laio, A.; VandeVondele, J.; Rothlisberger, U. *J. Phys. Chem. B* **2002**, *106*, 7300−7307.

(42) Becke, A. D. *Phys. Rev. A* **1988**, *38*, 3098.

(43) Lee, C.; Yang, W.; Parr, R. G. *Phys. Rev. B* **1988**, *37*, 785.

(44) Marx, D.; Hutter, J. *Modern Methods and algorithms of quantum chemistry*; Grotendorst, J., Ed.; Vol. 1 of NIC series; John von Neumann Institute for Computing: Juelich, 2000; pp 301−349.

(45) Troullier, N.; Martins, J. L. *Phys. Rev. B* **1991**, *43*, 1993.

(46) Amadei, A.; Linssen, A. B. M.; Berendsen, H. J. C. *Proteins* **1993**, *17*, 412−425.

(47) Garcia, A. E. *Phys. Rev. Lett.* **1992**, *68*, 2696−2699.

(48) Marzari, N.; Vanderbilt, D. *Phys. Rev. B* **1997**, *56*, 12847−12865.

(49) Rawlings, N. D.; Tolle, D. P.; Barrett, A. J. *Nucleic Acids Res.* **2004**, *32*, 160−164.

(50) Sharma, M.; Resta, R.; Car, R. *Phys. Rev. Lett.* **2007**, *98*, 247401.

(51) Tonge, P. J.; Carey, P. R. *Biochemistry* **1990**, *29*, 10723−10727.

(52) Tonge, P. J.; Carey, P. R. *Biochemistry* **1992**, *31*, 9122−9125.

(53) Carey, P. R. *Chem. Rev.* **2006**, *106*, 3043−3054.

(54) Perryman, A. L.; McCammon, J. A.; J. H. L. *Protein Sci.* **2004**, *13*, 1108−1123.